

RESULTS CONCERNING THE DECAY  $D_s^\pm \rightarrow \eta' \pi^\pm$ 

M.P. Alvarez<sup>2)</sup>, R. Barate<sup>3,b)</sup>, D. Bloch<sup>9)</sup>, P. Bonamy<sup>7)</sup>, P. Borgeaud<sup>7)</sup>, M. Burchell<sup>4)</sup>,  
H. Burmeister<sup>3)</sup>, J.M. Brunet<sup>6)</sup>, F. Calvino<sup>2,a)</sup>, M. Cattaneo<sup>4)</sup>, J.M. Crespo<sup>2)</sup>,  
B. d'Almagne<sup>5)</sup>, M. David<sup>7)</sup>, L. DiCiaccio<sup>3,c)</sup>, J. Dixon<sup>4)</sup>, P. Druet<sup>5)</sup>, A. Duane<sup>4)</sup>,  
J.P. Engel<sup>9)</sup>, A. Ferrer<sup>3,d)</sup>, T.A. Filippas<sup>1)</sup>, E. Fokitis<sup>1)</sup>, R.W. Forty<sup>4)</sup>, P. Foucault<sup>9)</sup>,  
E.N. Gazis<sup>1)</sup>, J.P. Gerber<sup>9)</sup>, Y. Giomataris<sup>3)</sup>, T. Hofmohl<sup>10)</sup>, E.C. Katsoufis<sup>1)</sup>,  
M. Koratzinos<sup>3,4,5)</sup>, C. Krafft<sup>5)</sup>, B. Lefevre<sup>6)</sup>, Y. Lemoigne<sup>7)</sup>, A. Lopez<sup>3,5,\*)</sup>, W.K. Lui<sup>8)</sup>,  
C. Magneville<sup>7)</sup>, A. Maltezos<sup>1)</sup>, J.G. McEwen<sup>8)</sup>, B. Pattison<sup>3)</sup>, D. Poutot<sup>6)</sup>,  
M. Primout<sup>7)</sup>, H. Rahmani<sup>1)</sup>, C. Seez<sup>4)</sup>, J. Six<sup>5)</sup>, R. Strub<sup>9)</sup>, D. Treille<sup>3)</sup>, P. Triscos<sup>6)</sup>,  
G. Tristram<sup>6)</sup>, G. Villet<sup>7)</sup>, A. Volte<sup>6)</sup>, M. Wayne<sup>5)</sup>, D.M. Websdale<sup>4)</sup>, G. Wormser<sup>5)</sup> and  
Y. Zolnierowski<sup>3)</sup>

## The NA14/2 Collaboration

(Submitted to Phys. Lett. B)

## Abstract

A search for the decay  $D_s^+ \rightarrow \eta' \pi^+$ ;  $\eta' \rightarrow \rho \gamma$  has been performed by the NA14/2 photoproduction experiment at CERN. A signal compatible with the  $D_s^+$  has been observed, leading to a ratio of branching fractions of:

$$\frac{\text{Br}(D_s^+ \rightarrow \eta' \pi^+)}{\text{Br}(D_s^+ \rightarrow \phi \pi^+)} = 2.5 \pm 1.0_{-0.4}^{+1.5}.$$

A value of  $\text{Br}(D^+ \rightarrow \eta' \pi^+)/\text{Br}(D^+ \rightarrow K^- \pi^+ \pi^+) < 0.1$  is set at 90% CL.

- 
- 1) National Technical University, Athens, Greece.
  - 2) Universidad Autónoma de Barcelona, Bellaterra, Spain.
  - 3) CERN, Geneva, Switzerland.
  - 4) Blackett Lab., Imperial College, London, UK.
  - 5) LAL, IN2P3-CNRS and Univ. Paris-Sud, Orsay, France.
  - 6) Collège de France, Paris, France.
  - 7) DPhPE, CEN-Saclay, Gif-sur-Yvette, France.
  - 8) Univ. of Southampton, Southampton, UK.
  - 9) CRN, IN2P3-CNRS and Univ. L. Pasteur, Strasbourg, France.
  - 10) Univ of Warsaw, Warsaw, Poland.
  - a) Univ. Politècnica de Catalunya, ETSEIB-DEN, Barcelona, Spain.
  - b) Univ. J. Fourier and ISN, Grenoble, France.
  - c) Univ. di Roma II, 'Tor Vergata', Rome, Italy.
  - d) IFIC, Centro Mixto Univ. de Valencia-CSIC, Valencia, Spain.
  - \*) On leave from Fac. de Ciencias Físicas, Univ. Complutense, Madrid, Spain.

## 1. INTRODUCTION

Ten years of active experimental research on the  $D_s^+$  meson (throughout the paper, the charge-conjugate states are implicitly included) have revealed only a relatively small fraction of its properties. Its lifetime is now well measured [1, 2, 3], but many of its decay modes are not well measured. A coherent description of the interplay between the different mechanisms of hadronic decays—spectator decays, annihilation decays, final-state interactions—is still lacking, but their relative importance has been assessed. Stringent upper limits on the decays  $D_s^+ \rightarrow \rho\pi^+$  [4] and  $\omega\pi^+$  [5] indicate that annihilation cannot play an important role in  $D_s^+$  decays. The equality of the branching fractions  $D_s^+ \rightarrow \phi\pi^+$  and  $D_s^+ \rightarrow \bar{K}^{0*}K^+$  clearly shows the absence of the colour suppression mechanism.

The next striking feature in the known  $D_s^+$  decays is the smallness of the observed branching fractions. The pilot branching fraction,  $D_s^+ \rightarrow \phi\pi^+$ , is of the order of 3% [6] and most observed decays modes are comparable with or even smaller than this one. Vector-vector decays, generally thought to have large branching ratios, also seem to be rather modest as indicated by recent results on the  $\phi\pi^+\pi^0$  mode [5, 7]. The channel  $D_s^+ \rightarrow \eta'\pi^+$  has been reported [8] to have a large branching ratio,  $\text{Br}(D_s^+ \rightarrow \eta'\pi^+)/\text{Br}(D_s^+ \rightarrow \phi\pi^+)$ , which should be  $5 \pm 2.3$ . This paper is devoted to results for this channel.

## 2. EXPERIMENTAL APPARATUS

The NA14/2 set-up consists of a large-acceptance spectrometer that measures charged and neutral particles with a good precision, and a silicon microvertex detector for the selection and identification of charmed particles. It is described in greater detail elsewhere [9]. Only the microvertex detector and the forward electromagnetic calorimeter are of importance to the analysis described here.

The microvertex detector comprises an active target, made of 32 planes of silicon, each 300  $\mu\text{m}$  thick, and a silicon microstrip telescope, made of 10 planes of 50  $\mu\text{m}$  pitch strips. This set-up enables a resolution of about 300  $\mu\text{m}$  along the flight direction for the primary and the secondary vertices.

The forward electromagnetic calorimeter is a large lead-glass array, in association with a position detector made of 800 scintillators, each 1.5 cm wide, placed after  $3X_0$  of lead glass. The resolutions in energy and position of the calorimeter are respectively  $0.1\sqrt{E}$  GeV and 3 mm for a photon above 2 GeV.

## 3. SEARCH FOR $D_s^+ \rightarrow \eta'\pi^+$

This decay was searched for, using the  $\eta' \rightarrow \rho\gamma$  decay mode, which gives a final configuration of three charged tracks and one photon. The three tracks have to form a detached vertex, while only one photon is present in the  $D_s$  decay products, with a consequent high detection efficiency. This decay mode is thus easier to observe than others. As an example, the  $\eta\pi^+\pi^-$  decay mode, with  $\eta \rightarrow \gamma\gamma$ , has a branching fraction two times smaller than the  $\rho\gamma$  one, a detection efficiency in our apparatus two times smaller and a higher background.

### 3.1 Data processing

The complete data set, 17 million events, containing  $\sim 2\%$  of charmed events, was first passed through a fast filter that selected events where at least one charged track is not compatible with a common primary vertex. The filter properties have been studied in great detail using the dominant decay modes of the D meson,  $D^0 \rightarrow K^-\pi^+$  and  $D^+ \rightarrow K^-\pi^+\pi^+$

[3, 7]. The efficiency of this filter, measured using an unfiltered data sample, is  $\approx 60\%$  for these decay channels, and is well reproduced by our Monte Carlo simulation. For the decay chain of interest here,  $D_s^+ \rightarrow \eta' \pi^+; \eta' \rightarrow \rho \gamma$ , it is found to be 68%, according to the Monte Carlo simulation.

This filter rejects 82% of the initial sample. All selected events were then completely reconstructed. A second selection procedure retained only those events where three charged tracks could form a detached secondary vertex. For each 3-prong combination, a common vertex was searched for and accepted if its  $\chi^2$  probability was above 1%. A primary vertex was then reconstructed, using the remaining charged tracks. If the  $\chi^2$  probability was too low for the vertex to be accepted, the track with the largest partial contribution was rejected and the process reiterated, with the requirement that at least two tracks form the primary vertex. Events were kept when they satisfied  $\Delta x / \sigma_x > 3$ , where  $\Delta x$  is the separation of the two vertices along the beam direction and  $\sigma_x$  the error associated to it. This selection procedure is the same as that used for the  $D^+ \rightarrow K^- \pi^+ \pi^+$  channel, where we have high statistics and can make consistency checks.

### 3.2 The $\eta' \pi^+$ signal

Using this sample, a dedicated search for  $D_s^+ \rightarrow \eta' \pi^+$  was then pursued. A detached 3-prong secondary vertex was required, to which each photon found in the forward electromagnetic calorimeter was added in turn to form a  $D_s^+$  candidate. The corresponding reconstructed  $D_s^+$  track was extrapolated back to the target and used to form the primary vertex. At least one other charged track was combined with the  $D_s^+$  track to form the primary vertex. All events with a  $\pi\pi\pi\gamma$  mass above  $1.6 \text{ GeV}/c^2$  were kept. A kinematical fit of the  $\eta'$  was performed when the raw  $\pi\pi\pi\gamma$  mass was found to lie between  $0.9$  and  $1.01 \text{ GeV}/c^2$ .

Finally, the following selection criteria were applied on the data :

- i) The photon energy has to be greater than  $2 \text{ GeV}$ .
- ii) The  $\pi^+ \pi^-$  pair forming the  $\rho$  candidate has a mass between  $0.6$  and  $0.8 \text{ GeV}/c^2$ . This range is well suited to the asymmetric line shape of the  $\rho$  resonance observed in the decay  $\eta' \rightarrow \rho \gamma$ .
- iii) None of the three charged tracks is identified as a K or a p by the Cherenkov counter.
- iv) The  $\chi^2$  probability of the primary vertex fit is greater than 10%. This cut rejects events where a large distance between the two vertices is due to a bad reconstruction of the primary vertex. This was checked by using the active target to measure the primary vertex position independently.

Figures 1a and 1b show the  $\pi\pi\pi\gamma$  mass spectra obtained after these cuts for events where the  $\pi\pi\pi\gamma$  mass is respectively inside the  $\eta'$  region ( $0.94\text{--}0.97 \text{ GeV}/c^2$ ) and outside it. A peak at the  $D_s^+$  mass is visible for the  $\eta'$  band, whilst the spectrum is smooth in the side-band regions. An  $\eta'$  signal is also visible (Fig. 2a) when the unfitted  $\pi\pi\pi\gamma$  mass is taken from the  $D_s^+$  region and is not present outside this region (Fig. 2b).

Several checks were made to assess the validity of the  $D_s^+$  signal:

- i) The signal was also visible when no kinematical fit was performed, although with a smaller statistical significance, as expected.
- ii) The photon was required not to belong to any  $\gamma\gamma$  combination forming a  $\pi^0$  candidate. Only 30% of the signal was lost, in good agreement with the random loss predicted by our simulation.
- iii) The track of opposite charge to the  $D_s^+$  was asked to be positively identified as

a pion or a kaon. The signal was only visible for identified pions. This result, in conjunction with the previous one, eliminates possible kinematic reflections from  $D^+$  or  $D^{*+}$  decays.

Although both cuts (ii) and (iii) tend to improve the signal-to-noise ratio, they are not used in the final analysis because of the relatively large uncertainties in their correction.

The solid curve shown in Fig. 1a is obtained by a fit to the mass distribution with a Gaussian of fixed width centred on the  $D_s^+$  mass combined with a shape of the background extracted from a fit on Fig. 1b. We obtain a number of  $D_s^+$  events of  $35 \pm 11$ . The same procedure was applied with a Gaussian centred at the  $D^+$  mass, where no signal is visible, and an upper limit of 10 events at the 90% CL is obtained.

#### 4. STUDY OF THE LIFETIME DISTRIBUTION

In order to extract the number of events and the lifetime of our signal simultaneously, we performed a two-dimensional fit to the mass and lifetime distributions, using the maximum-likelihood technique. This method was found to be less sensitive to background description than the independent estimation of the number of  $D_s^+$  events and of the  $D_s^+$  lifetime. We used the following normalized function:

$$\wp(m, t) = \varepsilon \frac{1}{\tau_{D_s}} \cdot e^{-t/\tau_{D_s}} \cdot \frac{1}{\sigma\sqrt{2\pi}} \cdot e^{-(m-m_0)^2/2\sigma^2} + (1 - \varepsilon) \wp_{\text{back}}^t(t) \wp_{\text{back}}^m(m),$$

where  $\varepsilon$  is the proportion of  $D_s^+$  events giving rise to the corresponding number  $N_{D_s}$ . Concerning the background, we took a parabolic form for the mass term; for the time-dependent term, we considered three contributions, as in our previous determinations of the lifetime of other charmed particles [3]: two exponentials and a flat term. The first short-lived exponential corresponds to single-vertex events and the second one to charmed-background events. The flat term is assumed to come from hadronic secondary interactions in the silicon active target.

The background parameters were fitted using the events outside the  $\eta'$  region of Fig. 1b. We found:

$$\tau_{b_1} = 0.06 \pm 0.01 \text{ ps}, \quad \tau_{b_2} = 0.24 \pm 0.05 \text{ ps},$$

and the relative abundance of each term was found to be 54% and 41% for the two exponentials and 5% for the flat term.

Fixing these background parameters, we fitted the function  $\wp(m, t)$  to the sample of events of Fig. 1a. The width  $\sigma$  was fixed to the value obtained by our Monte Carlo simulation. This fit with the two parameters  $\tau_{D_s}$  and  $\varepsilon$  gave the following results :

$$\begin{cases} \tau_{D_s} = 0.28 \pm 0.15 \text{ ps} \\ \varepsilon = 0.03 \pm 0.01 \end{cases}$$

giving  $N_{D_s} = 22 \pm 7.5$ .

If  $\tau_{D_s}$  was fixed to its nominal value of 0.436 ps [10],  $N_{D_s} = 20 \pm 7.5$  would be obtained. We have checked that our results are stable with respect to the variations of the background parameters in their allowed range.

Clearly, the two ways of determining  $N_{D_s}$ , i.e. without and with lifetime consideration, give different results:  $N_{D_s} = 35 \pm 11$  and  $N_{D_s} = 22 \pm 7.5$ ; this can be seen in the two

corresponding curves of Fig.1a. No clear explanation has been found for this difference. A statistical fluctuation in the mass distribution shown in Fig. 1a or in the lifetime distribution is possible. An incorrect description of the time distribution of the background could also contribute to such effects. We take the number  $ND_s = 22 \pm 7.5_{-2}^{+13}$ , where we added to the statistical error a systematic error covering our extreme numbers.

## 5. BRANCHING RATIO

To obtain the ratio  $\text{Br}(D_s^+ \rightarrow \eta' \pi^+) / \text{Br}(D_s^+ \rightarrow \phi \pi^+)$ , we determined our  $\eta' \pi^+$  efficiency with a Monte Carlo and used the results of our  $D_s^+ \rightarrow \phi \pi^+$  analysis [7]. In such a ratio, many systematic uncertainties related to trigger, detector, and filter efficiencies cancel out. The main source of systematic error is in the estimation of  $N(D_s^+ \rightarrow \eta' \pi^+)$ . Other sources of systematic errors are the uncertainty in the  $\phi \pi$  detection efficiency, which is due to the limited energy range of K recognition in the detector, the uncertainty in the photon detection efficiency, and that in the mass resolution of the  $D_s^+$ .

Taking into account the branching fractions of 0.495 for  $\phi \rightarrow K^+ K^-$  and 0.301 for  $\eta' \rightarrow \rho \gamma$  [6], we derived :

$$\frac{\text{Br}(D_s^+ \rightarrow \eta' \pi^+)}{\text{Br}(D_s^+ \rightarrow \phi \pi^+)} = 2.5 \pm 1.0_{-0.4}^{+1.5} .$$

In a similar treatment, the absence of  $D^+ \rightarrow \eta' \pi$  led to the 90% CL limit :

$$\frac{\text{Br}(D^+ \rightarrow \eta' \pi^+)}{\text{Br}(D^+ \rightarrow K^- \pi^+ \pi^+)} < 10\% .$$

## 6. CONCLUSION

A signal compatible with the decay  $D_s^+ \rightarrow \eta' \pi^+$  has been observed using the  $\eta' \rightarrow \rho \gamma$  mode, from which the following ratio was derived:

$$\frac{\text{Br}(D_s^+ \rightarrow \eta' \pi^+)}{\text{Br}(D_s^+ \rightarrow \phi \pi^+)} = 2.5 \pm 1.0_{-0.4}^{+1.5} .$$

This result, slightly higher than some limits [10], is in agreement with a recent result [11]. It suggests that the  $\eta' \pi$  mode is an important decay mode of the  $D_s^+$  meson.

## REFERENCES

- [1] J.R. Raab et al. (Tagged Photon Spectrometer Collaboration), Phys. Rev. **D37** (1988) 2391.
- [2] H. Becker et al. (ACCMOR Collaboration), Phys. Lett. **B184** (1987) 277.
- [3] M.P. Alvarez et al. (NA14/2 Collaboration), Z. Phys. **C47** (1990) 539.
- [4] J.C. Anjos et al., Phys. Rev. Lett. **62** (1989) 125.
- [5] J.C. Anjos et al., Phys. Lett. **B223** (1989) 267.
- [6] G.P. Yost et al., Particle Data Group, Phys. Lett. **B239** (1990) 1.
- [7] M.P. Alvarez et al. (NA14/2 Collaboration), Phys. Lett. **B246** (1990) 261.
- [8] G. Wormser et al., Phys. Rev. Lett. **61** (1988) 1057.
- [9] P. Astbury et al., Phys. Lett. **152B** (1985) 419.  
R. Barate et al., Nucl. Instrum. Methods **A233** (1985) 235.  
G. Barber et al., Nucl. Instrum. Methods **A253** (1987) 530.
- [10] G. Gladding (Mark III Collaboration), presented at the Symposium on Heavy Quarks Physics, Cornell University, 1989.  
P.E. Karchin (E691 Collaboration), presented at the XIV Int. Symposium on Lepton and Photon Interactions, Stanford University, 1989.
- [11] H. Albrecht et al. (ARGUS Collaboration), Phys. Lett. **B245** (1990) 315.

## FIGURE CAPTIONS

- Fig. 1 :**  $\pi^+\pi^-\pi^\pm\gamma$  mass distribution (a) for the  $\pi^+\pi^-\gamma$  mass in the  $\eta'$  region (b) for the  $\pi^+\pi^-\gamma$  mass outside the  $\eta'$  region, as explained in the text. The solid curves correspond to fits on the mass distribution, the dashed curve in (a) is a combined fit to mass and lifetime.
- Fig. 2 :**  $\pi^+\pi^-\gamma$  mass distribution for the  $\pi^+\pi^-\pi^\pm\gamma$  mass (a) inside  $D_s^+$  region and (b) outside it.

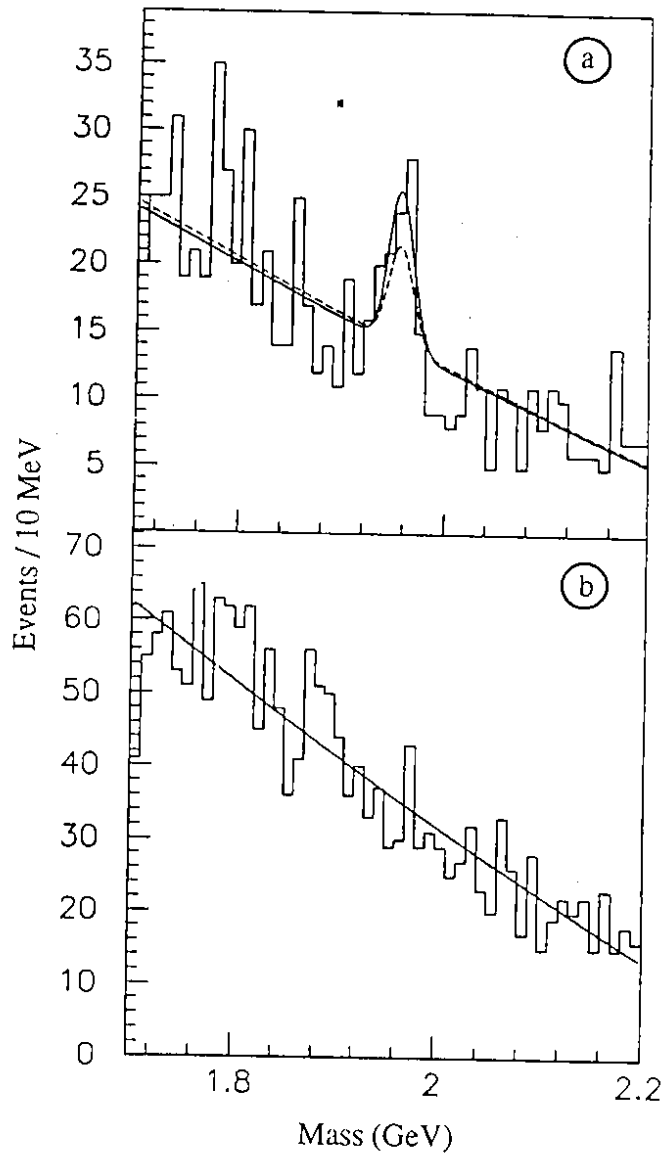


Fig. 1

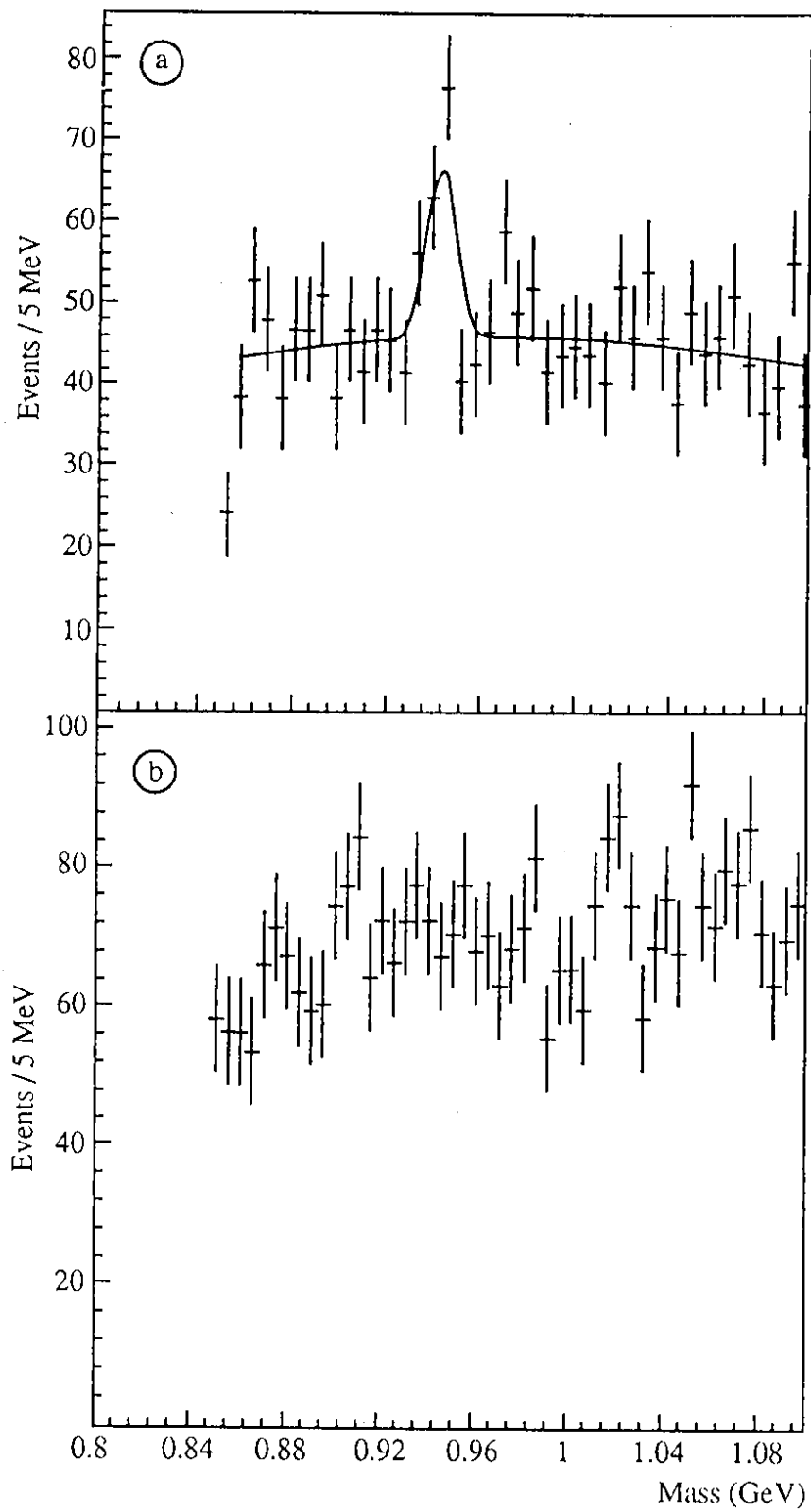


Fig. 2